Multimode Strong Coupling in Cavity Optomechanics

P. Kharel, Y. Chu, D. Mason, E. A. Kittlaus, N. T. Otterstrom, S. Gertler, and P. T. Rakich

Phys. Rev. Applied **18**, 024054 — Published 19 August 2022

DOI: 10.1103/PhysRevApplied.18.024054

Multimode strong coupling in cavity optomechanics

P. Kharel[†],[1,*] Y. Chu,[1,2] D. Mason,[1] E. A. Kittlaus,[1] N. T. Otterstrom,[1] S. Gertler,[1] and P. T. Rakich[1]

[1]*Department of Applied Physics, Yale University, New Haven, Connecticut 06511, USA and Yale Quantum Institute, Yale University, New Haven, Connecticut 06520, USA*
[2]*Department of Physics, ETH Zürich, 8093 Zürich, Switzerland and Quantum Center, ETH Zürich, 8093 Zürich, Switzerland*[†]

Optomechanical systems show great potential as quantum transducers and information storage devices for use in future hybrid quantum networks. In this context, optomechanical strong coupling can enable efficient, high bandwidth, and deterministic transfer of quantum states. While optomechanical strong coupling has been realized at optical frequencies, it has proven difficult to identify a robust optomechanical system that features the low loss and high coupling rates required for more sophisticated control of mechanical motion. In this paper, we demonstrate strong coupling in a Brillouin-based bulk cavity optomechanical system in both the single and multimode strong coupling regime, which leads to a useful device for both applications in quantum information and for investigating decoherence phenomenon in bulk acoustic wave resonators. Using nontrivial mode hybridizations in the strong coupling regime, we create hybridized photonic-phononic modes with lifetimes that are significantly longer than those of the uncoupled system. This surprising lifetime enhancement, which results from the interference of decay channels, showcases the use of multimode strong coupling as a general strategy to control extrinsic decoherence mechanisms. Moreover, phonons supported by such BAW resonators have a collection of properties, including high frequencies, long coherence times, and robustness against thermal decoherence, making this optomechanical system particularly enticing for applications such as quantum transduction and memories. Hence, this system provides access to phenomena in a previously unexplored regime of optomechanical interactions and could serve as an important building block for future quantum devices.

I. INTRODUCTION

As is the case for many quantum-optical systems, optomechanical devices exhibit novel physical behaviors and acquire new useful capabilities when they enter the so-called "strong coupling regime" [1]. In this regime, the coupling rate between light and motion becomes faster than both the optical and mechanical dissipation rates, which is necessary for applications such as quantum transduction [2, 3] and memories [4, 5]. Since light is the natural carrier of quantum information over long distances [6], and mechanical motion efficiently couples to many quantum systems [7–9], a robust and coherent interface between light and mechanical motion could be a useful building block in hybrid quantum networks for long-distance communications [10] or modular quantum computation [11]. In such systems, strong coupling permits operation in the regime where transduction bandwidth can be maximized. Beyond quantum communication, strong coupling is also necessary for applications that seek to utilize the information stored in the optical mode[12] rather than released from the cavity such as in hybrid quantum systems where light is coupled to individual atoms or quantum dots [13, 14].

Only a few optomechanical devices have entered the regime of optomechanical strong coupling due to technical challenges associated with realizing low-loss systems that can also robustly support high coupling rates. Radiation pressure has been used to achieve strong coupling between THz-frequency optical modes and MHz-frequency mechanical modes within micromechanical systems [15, 16]. However, if we seek to utilize optomechanical systems as a quantum resource, it is advantageous to instead utilize high frequency (GHz) phonon modes; this is because higher frequencies yield lower thermal decoherence at any given temperature, enable faster quantum operations, and allow access to the mechanical ground state using standard refrigeration techniques. Despite the many successes of GHz-frequency micro- and nano-optomechanical systems [17], it remains challenging to reach strong coupling in such systems due to practical limits [18, 19] on the circulating photon number, which in turn limit the cavity-enhanced coupling rate.

Through an alternative approach, Brillouin interactions have been used to demonstrate strong coupling to GHz-frequency mechanical modes of a fused-silica whispering gallery mode resonator [20]. This strategy permits resonant driving of the optical mode, and the use of macroscopic fused-silica based resonators having low material- and surface-induced absorption alleviates some of the technical challenges associated with laser heating, making large coupling rates more readily accessible. While this recent demonstration illustrates the advantages of Brillouin-based coupling in macroscopic systems, low acoustic dissipation rates–necessary to store information in the mechanical mode–are difficult to achieve in glasses at cryogenic temperatures. In particular, two-level tunnelling-state systems, which are intrinsic to silica, produce excess dissipation and noise at cryogenic

* prashanta.kharel@gmail.com
† These two authors contributed equally.

temperatures [21, 22], complicating the prospects for efficient quantum operations in such systems. However, a promising way to address this challenge could be to realize strong coupling between optical cavity modes and the long-lived high-frequency (>10 GHz) phonon modes supported by crystalline bulk acoustic wave (BAW) resonators [23].

Separate from the opportunities presented by strong coupling, another direction with significant untapped potential in cavity optomechanics–more generally in quantum information science–involves the exploration of coupled multimode systems. Such systems have already given rise to the observation of a wide variety of interesting physical phenomena, such as optomechanical dark modes [24, 25], synchronization of mechanical frequencies [26], topological dynamics [27], and non-reciprocity [28]. Achieving strong coupling within a multimode system could lead to a wealth of new capabilities including storage of light through control of bright and dark states [29] and exploration of topological phonon transport [30, 31]. Furthermore, in the quantum regime, multimode strong coupling could open the door to generation of multipartite mechanical entanglement [32–34] and the implementation of a quantum simulator for many-body bosonic systems [35, 36].

In this paper, we utilize Brillouin interactions to demonstrate strong coupling between a single optical mode and one or more high-frequency (12.6 GHz) modes of a crystalline bulk acoustic resonator at cryogenic temperatures. Our system combines a high-finesse optical resonator with a low-loss, crystalline BAW resonator, which can be reconfigured so that the optical mode is strongly coupled to either a single acoustic mode or several acoustic modes. Using both frequency and time-domain measurements, we quantify the parameters of the system and explore its dynamics. In the single mode case, we achieve an optomechanical coupling rate of $g_{\mathrm{m}} = 2\pi \times (7.2 \pm 0.1)$ MHz, which exceeds both the optical dissipation rate of $\kappa = 2\pi \times (4.43 \pm 0.02)$ MHz and the mechanical dissipation rate of $\Gamma_{\mathrm{m}} = 2\pi \times (66 \pm 3)$ kHz. In the multimode case, the coupling rates exceed the acoustic free spectral range of $\delta = 2\pi \times (610 \pm 10)$ kHz, meaning we enter the multimode strong coupling regime. In this regime, strong coupling produces a new set of optomechanical "dark modes" with linewidths that are a factor of five less than the smallest dissipation rate, Γ_{m}, of the uncoupled system. We show that this intriguing phenomenon can be explained by the destructive interference of radiative loss channels for the dark modes.

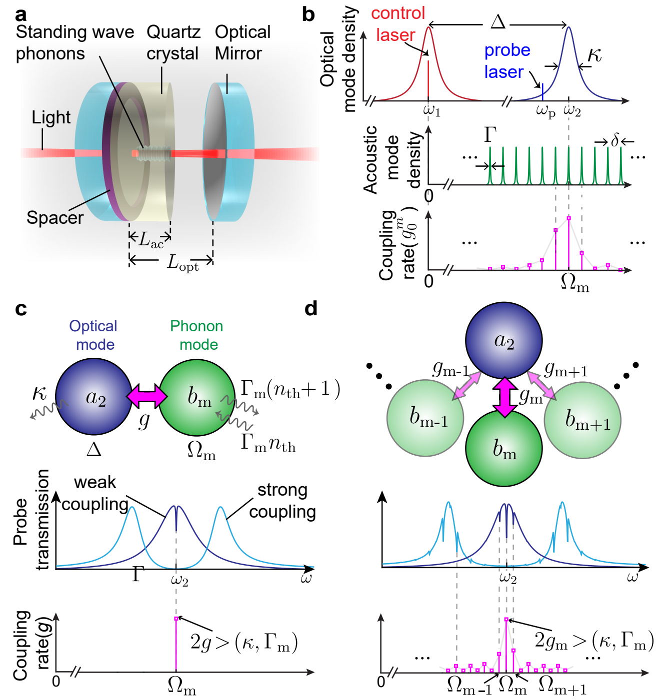

Figure 1. Multimode cavity optomechanical system. (a) Schematic of the optomechanical system (not to scale). The thickness of the half-inch diameter quartz crystal is $L_{\mathrm{ac}} = 5$ mm and the spacing between the optical mirrors is $L_{\mathrm{opt}} = 9.9$ mm. The optical and acoustic mode waist diameter is 122 μm and 86 μm, respectively. (b) Schematic spectra of optical modes (top) and acoustic modes (middle). The zero-point optomechanical coupling rates (bottom) are determined by a combination of the Brillouin bandwidth dictated by energy and momentum conservation, and the spatial overlap of acoustic and optical modes [37]. (c) Diagram of linearized optomechanical coupling between an optical mode and a single acoustic mode (top), corresponding to expected spectra of probe laser transmission in the weak- and strong-coupling regime (middle), and coupling rate under a strong control laser drive (bottom). (d) Same as in (c) except the optical mode is coupled to many acoustic modes. Here, the coupling to one acoustic mode is dominant, corresponding to the case in Figures 2 and 3.

II. CAVITY OPTOMECHANICAL SYSTEM

Our optomechanical system consists of a planar quartz crystal that is placed within a Fabry-Pérot optical cavity with high reflectivity (99.9%) optical mirrors (Fig. 1a). At a temperature of ~ 10 K, long-lived longitudinal acoustic modes within the quartz crystal are reflected from the planar surfaces of the crystal to form a series of macroscopic standing wave acoustic modes similar to the standing wave electromagnetic modes formed within a Fabry-Pérot optical cavity. A high-frequency acoustic mode within the BAW resonator (formed by the quartz crystal) can mediate coupling between two distinct longitudinal modes of the optical cavity through Brillouin interactions when energy conservation and phase matching requirements are satisfied (Fig. 1b). For crystalline z-cut quartz at cryogenic temperatures and optical modes near 1550 nm, such interactions occur for a narrow band of acoustic modes near 12.6 GHz (see Supplementary Information section I [38]).

This multimode coupling can be described by the in-

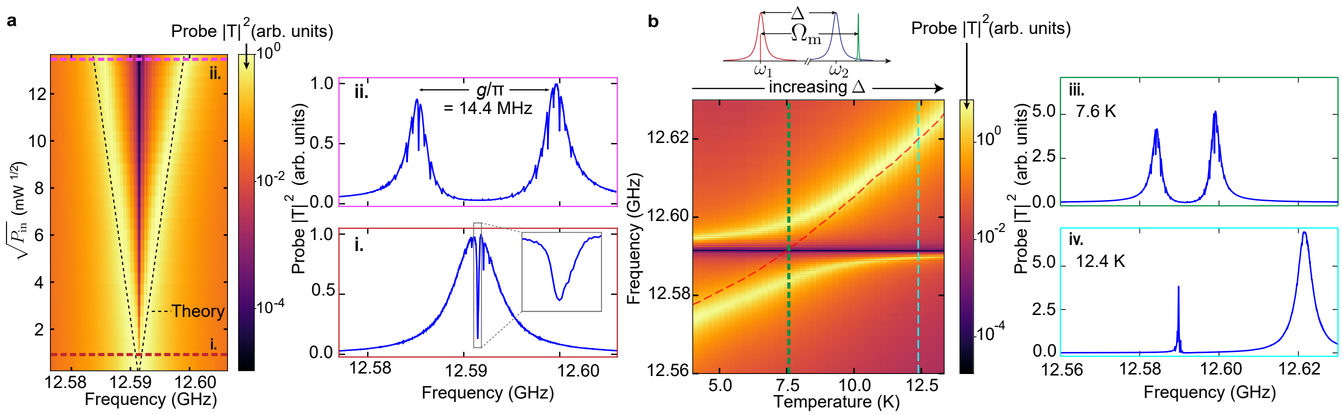

Figure 2. **Optomechanical strong coupling to a single mechanical mode.** (a) Probe laser transmission spectra taken at various control laser powers. Dashed lines show expected values of g_{m} for the dominantly coupled acoustic mode, extrapolated from fits to low-power spectra with $\sqrt{P_{\mathrm{in}}} < 0.6\ \mathrm{mW}^{1/2}$ (see Supplementary Information section II [38]). Lower and upper panels (inset **i - ii**) show spectra in the regimes of weak and strong coupling, respectively. In the strongly coupled case, the normal-mode splitting indicated is due to the dominantly-coupled acoustic mode, but OMIT features are visible from other acoustic modes that are still weakly coupled. (b) Probe transmission taken at various cryostat temperatures. Dashed red line shows the value of Δ at each temperature, obtained by fitting the data to the theoretical expression for probe transmission (see Supplementary Information section II [38]). Panels (inset **iii - iv**) show spectra in the resonant and far-detuned cases.

teraction Hamiltonian

$$H_{\mathrm{int}} = -\sum_{\mathrm{m}} \hbar g_0^{\mathrm{m}} (a_2^\dagger a_1 b_{\mathrm{m}} + a_1^\dagger a_2 b_{\mathrm{m}}^\dagger), \qquad (1)$$

where $a_1^\dagger$ ($a_2^\dagger$) is the creation operator for the optical mode at frequency ω_1 (ω_2), $b_{\mathrm{m}}^\dagger$ is the creation operator for the acoustic mode at frequency Ω_{m}, and g_0^{m} is the zero-point coupling rate. We note that g_0^{m} depends on the spatial acousto-optical overlap, which provides us with a way of tailoring the optomechanical coupling strength for different acoustic modes [37]. With an external control laser that is driven on resonance with the lower frequency optical mode a_1, we can write an effective linearized Hamiltonian as

$$H_{\mathrm{eff}} = \hbar\Delta a_2^\dagger a_2 + \sum_{\mathrm{m}} \hbar\Omega_{\mathrm{m}} b_{\mathrm{m}}^\dagger b_{\mathrm{m}} - \sum_{\mathrm{m}} \hbar g_{\mathrm{m}} (a_2^\dagger b_{\mathrm{m}} + a_2 b_{\mathrm{m}}^\dagger). \qquad (2)$$

Here, we have moved to the rotating frame of mode a_1, $g_{\mathrm{m}} = \sqrt{\bar{n}_{\mathrm{c}}} g_0^{\mathrm{m}}$ is the cavity-enhanced coupling rate, $\bar{n}_c$ is the intra-cavity photon number of mode a_1, and $\Delta = \omega_2 - \omega_1$ is the optical free spectral range.

The above beam-splitter Hamiltonian $\hbar g_{\mathrm{m}}(a_2^\dagger b_{\mathrm{m}} + a_2 b_{\mathrm{m}}^\dagger)$ describes coherent energy exchange between a single optical mode a_2 and a single acoustic mode b_{m} with interaction rate $2g_{\mathrm{m}}$. However, the dissipation rates relative to this interaction rate determine the optical transmission spectrum of mode a_2, which we measure using a weak probe field. In the weak coupling regime $g_{\mathrm{m}} < (\kappa/2, \Gamma_{\mathrm{m}}/2)$, we expect a narrow dip in the transmission spectrum due to the well known phenomenon of optomechanically induced transparency (OMIT) [39] seen in Fig. 1c. In the strong coupling regime $g_{\mathrm{m}} > (\kappa/2, \Gamma_{\mathrm{m}}/2)$, the optical transmission spectrum develops two resonant features that correspond to new modes that result from the hybridization between the optical mode a_2 and the individual mechanical mode b_{m} seen in Fig. 1c.

Because our experimental system permits coupling to an array of acoustic modes, the optical mode spectrum develops additional features in the strong coupling regime. Since a BAW resonator supports multiple acoustic modes with regular frequency spacing (δ) that is smaller than the optical dissipation rate (κ), it is important to go beyond the minimal model of a single optical mode coupled to a single phonon mode. This is because, more than one acoustic modes can simultaneously mediate coupling between the same pair of optical modes (Fig. 1b). Therefore, in addition to normal-mode splitting of a single strongly coupled acoustic mode (Ω_{m}), we expect several OMIT dips to arise from weak coupling to a multitude of acoustic modes (e.g. $\Omega_{\mathrm{m}-2}, \Omega_{\mathrm{m}-1}, \Omega_{\mathrm{m}+1}, \Omega_{\mathrm{m}+2}$) as seen in Fig. 1d.

III. EXPERIMENTAL RESULTS

A. Strong coupling to a single acoustic mode

We first present experimental measurements of strong optomechanical coupling when our system is configured to couple predominantly to a single acoustic mode. For the lowest control laser power, the transmission spectrum seen in Fig. 2a.i reveals a single OMIT dip at $\Omega_{\mathrm{m}} = 2\pi \times 12.591$ GHz. Through these low power measurements in the weak coupling regime, we extract $\kappa = 2\pi \times (4.43 \pm 0.02)$ MHz, $\Gamma_{\mathrm{m}} = 2\pi \times (66 \pm 3)$ kHz, and $g_0^{\mathrm{m}} = 2\pi \times (23 \pm 1)$ Hz (See Supplementary Information section II [38]). Note that the asymmetric line shape seen in Fig. 2i (inset) is characteristic of leaky modes supported by flat-flat resonator geometries (See Supplementary Information section V.A [38]). To reach the regime of strong coupling, we enhance g_{m} by increasing $\bar{n}_{\mathrm{c}}$. As expected from theory, we observe a normal-mode splitting that increases proportional to $\sqrt{P_{\mathrm{in}}}$ (Fig. 2a), where P_{in} is the input control laser power.

As another unambiguous signature of strong coupling, we tune the FSR of the optical cavity modes into and out of resonance with the strongly coupled acoustic mode to reveal a characteristic anticrossing feature (Fig. 2b). Because the optical mode spacing, Δ, depends on the temperature, T, we can readily tune Δ to match the frequency, Ω_{m}, of Brillouin-active phonon modes. During these measurements, we lock the control laser on resonance with the optical mode at ω_1, such that temperature tuning allows us to change optical mode spacing, Δ, without changing g_{m}. From transmission spectra obtained as a function of T at the highest control power, we observe a clear anticrossing at $T = 7.6$ K when $\Delta \simeq \Omega_{\mathrm{m}}$ (Fig. 2b.i). For the off-resonant case ($\Delta \neq \Omega_{\mathrm{m}}$) at $T = 12.4$ K, we obtain a narrow and a broad resonance features seen in Fig. 2b.ii, which correspond to the acoustic and the optical modes of the uncoupled system, respectively.

At the highest P_{in} of 187 mW, corresponding to an intracavity photon number $\bar{n}_{\mathrm{c}} = 1.1 \times 10^{11}$, we observe a splitting $2g_{\mathrm{m}} = 2\pi \times (14.4 \pm 0.1)$ MHz (Fig. 2a.ii). Since $2g_{\mathrm{m}}/\kappa \simeq 3$ and $2g_{\mathrm{m}}/\Gamma_{\mathrm{m}} \simeq 220$, the coherent coupling rate far exceeds the dissipation rates of both the optical and the acoustic modes, indicating that our system is in the strong coupling regime. For mechanical oscillators with non-zero thermal occupations, it is relevant to consider not only how the coupling rate compares to the dissipation rates, but also to the total (thermal) decoherence rate, $\gamma_{\mathrm{th}} = n_{\mathrm{th}}\Gamma_m$. In this way, one can define the quantum cooperativity, $C_q = 4g_{\mathrm{m}}^2/\kappa\gamma_{\mathrm{th}}$. Achieving $C_q > 1$ indicates that quantum state transfer between photons and phonons can occur at a much faster rate than the mechanical decoherence. This opens the door for many quantum-coherent protocols, including efficient and low-noise quantum transduction of information between the optical and acoustic domain [40, 41].

To characterize γ_{th} (and thus C_q), one must measure the mechanical bath occupation, which we accomplish through a series of calibrated thermometry measurements of undriven thermal motion. By carefully characterizing our optical detection path with an optical calibration tone, and extracting optomechanical scattering rates with a driven measurement, we can reliably calibrate measured RF voltage spectra into units of mechanical quanta necessary to extract the effective phonon occupation number (see Supplementary Information section III for details [38]). From these measurements, we extract a thermal bath occupation of $n_{\mathrm{th}} = 25 \pm 1$, yielding a thermal decoherence rate of $2\pi \times (1.6 \pm 0.1)$ MHz.

To apply standard methods for estimation of the thermal occupation (including the effects of sideband cooling) [42], it was necessary to perform measurements of thermal occupation at lower coupling rates. However, to understand our prospects for reaching high quantum cooperativities, we must investigate the possibility of spurious mode heating at higher powers (and higher coupling rates). Absorbed light has been observed to cause excessive heating of the mechanical mode [18, 41], limiting the performance of state-of-the-art quantum optomechanical experiments [2, 43]. By comparison, this bulk crystalline system has several properties that could prove advantageous in this regard. For example, the high-purity quartz crystals used within our optomechanical system have exceedingly low material absorption [44]. At the same time, the macroscopic crystalline substrate has high thermal conductivity (>20 W cm^{-1} K^{-1}) which peaks around 10 Kelvin [45] and also has good thermal anchoring to the cryostat, helping to minimize any temperature changes produced by any deposited heat. To quantify the degree of possible laser heating, we repeat our calibrated thermometry experiments in the presence of an auxiliary 'heating laser' that is used to drive a separate optical mode (not participating in the optomechanical process). Within the uncertainty of our measurements, we observe that the presence of a strong heating laser does not alter the thermal decoherence rate of the mechanical mode at input optical powers of 150 mW, which is comparable with the highest control laser powers used to demonstrate strong coupling (see Supplementary Information section III for details [38]).

These measurements confirm that we can reach optomechanical scattering rates ($4g_{\mathrm{m}}^2/\kappa$) which exceed the thermal decoherence rate (γ_{th}) by over an order of magnitude, corresponding to the regime of strong quantum cooperativity (or $C_q > 1$). With the parameters demonstrated here, ground-state sideband cooling experiments should be straightforward, though one must carefully manage and model the multimode interactions and coupled dissipation channels. In this direction, it may be more straightforward to work with a plano-convex crystal [23], which offers a higher acoustic finesse, such that multimode interactions are less relevant.

Next we demonstrate time-domain control and utilize it to study the dynamics of our system under a pulsed probe signal. These pulsed operations are not only an important step toward implementing deterministic state transfer for quantum transduction and information storage, but also allow us to perform accurate measurements of the timescales for coherent and dissipative dynamics within our optomechanical system [41]. We probe the time domain dyamics of our system by pulsing a weak probe light (ω_2) while maintaining a strong continuous drive at ω_1 (Fig. 3a). A heterodyne signal resulting from the interference between the control and the probe light transmitted through the cavity provides phase-sensitive detection of the probe light as a function of time (See Supplementary Information section I [38]).

The temporal response observed using this method help to elucidate some subtle features that emerge from multimode strong coupling. These time-domain measurements, shown in Fig. 3b, were performed at the

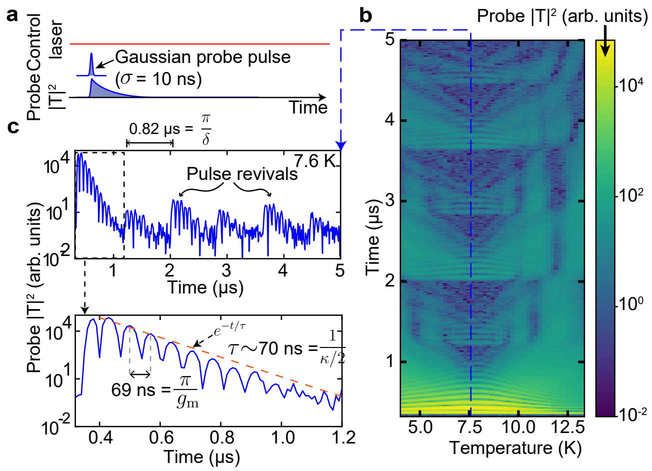

Figure 3. Time-domain measurements of strong coupling. (a) Schematic of the time-domain measurement. A strong control laser is continuously on-resonance with the optical mode at ω_1 to turn on the optomechanical coupling (see Fig. 1b). A short probe pulse excites the optical mode at $\omega_2 = \omega_1 + \Omega_{\mathrm{m}}$ and the response of the system is then recorded as a function of time (see Supplementary Information section I [38]). (b) Time-domain measurements taken at the same set of cryostat temperatures as in Fig. 2b. Note that in these measurements, the probe frequency is centered at Ω_{m}, but has a large enough bandwidth to excite the optical mode even when it is detuned. (c) Probe transmission as a function of time after probe pulse is turned on (top) and zoom in (bottom) showing oscillations at π/g_{m} and exponential decay with timescale $\tau \sim 2/\kappa$.

same temperatures as the frequency-domain measurements shown in Fig. 2b, and result in a characteristic detuning dependency of Rabi oscillations obtained when two resonators coherently exchange energy in the strong coupling regime [46]. At $T = 7.6$ K (when $\Delta \simeq \Omega_{\mathrm{m}}$), we observe coherent oscillations with a period of 69 ns, which is consistent with the value of $2g_{\mathrm{m}}$ extracted from frequency domain measurements. As seen in Fig. 3c the time constant τ for this energy decay is 70 ns, which agrees well with the energy decay rate of $(\kappa + \Gamma_{\mathrm{m}})/2 \approx \kappa/2$ of the hybridized modes. Notice, however, that additional revivals of the coherent oscillations are observed for $t \gg \tau$ in Fig. 3c. These nontrivial features appear because the spectrally-broad probe pulse excites a single strongly coupled acoustic mode as well as a multitude of weakly coupled acoustic modes that lie outside the phase matching bandwidth. These results are consistent with multiple OMIT dips that arise from weak coupling to multiple acoustic modes in the spectral domain as seen in Fig. 2a. Due to the modulation in the coupling strength produced by the overlap between optical and acoustic modes within this device geometry, g_0^{m} is suppressed for alternating acoustic mode numbers m outside the phase matching bandwidth (Fig. 1d). For this reason, the observed revivals have a period of 0.82 μs, corresponding to a frequency of 1.2 MHz, which is approximately twice the acoustic free-spectral range of 610 kHz. Since the lifetimes of such weakly coupled modes approach the intrinsic mechanical decay time of the uncoupled system, $1/\Gamma_{\mathrm{m}} \simeq 2.4$ μs, the revivals are sustained for $t \gg \tau$.

B. Strong coupling to multiple acoustic modes

So far, we have demonstrated robust strong coupling between a single optical mode and a single high frequency acoustic mode in our Brillouin-based bulk cavity optomechanical system. Next, we show that this system can be reconfigured to achieve multimode strong coupling regime, which leads to useful device physics for both applications in quantum information and investigating decoherence phenomena in bulk acoustic resonators. To enter the multimode strong coupling regime, we strongly couple a single optical mode to three acoustic modes (Fig. 4a). We accomplished this by tuning the optical wavelength to select a different pair of optical modes, which changes the spatial overlap between the optical and acoustic modes (See Supplementary Information section I [38]). The transmission spectrum taken at low power (Fig. 4b.i) reveals three OMIT dips. As before, theoretical fits to OMIT spectrum at low powers allow us to extract coupling rates $g_1 = 2\pi \times (4.9 \pm 0.1)$ MHz, $g_2 = 2\pi \times (4.0 \pm 0.1)$ MHz and $g_3 = 2\pi \times (3.7 \pm 0.1)$ MHz, as well as dissipation rates $\kappa = 2\pi \times (2.52 \pm 0.08)$ MHz and $\Gamma_{\mathrm{m}} = 2\pi \times (67 \pm 10)$ kHz (See Supplementary Information section II [38]). In the strong coupling regime, we observe four distinct peaks in the transmission spectrum seen in Fig. 4b.ii. These peaks represent the four eigenmodes produced by the hybridization of the optical mode (a_2) with the three dominant phonon modes b_1, b_2, and b_3.

To understand the nature of these four new eigenmodes, we start by considering a simpler case of a single optical mode (a_2) coupled strongly to two phonon modes (b_1, b_2) separated by 2δ. Furthermore, we assume that $g_1 = g_2 \equiv g$, $\Gamma_1 = \Gamma_2 \equiv \Gamma$, and $\Omega_{1,2} = \Delta \mp \delta$. The Hamiltonian of this three coupled oscillator system in the basis of a_2, b_1, and b_2 is given by

$$H_{\mathrm{eff}} = \begin{bmatrix} \Delta - i\kappa/2 & -g & -g \\ -g^* & \Omega_1 - i\Gamma/2 & 0 \\ -g^* & 0 & \Omega_2 - i\Gamma/2 \end{bmatrix}. \quad (3)$$

This effective Hamiltonian can be diagonalized to obtain three eigenmodes of the hybridized system (see Supplementary Information section V [38]). In the limit of large g, these eigenmodes become two 'bright' modes $B_\pm = \frac{1}{\sqrt{2}} a_2 \pm \frac{1}{2}(b_1 + b_2)$ at frequencies $\omega_\pm = \Delta \pm \sqrt{2} g$ with dissipation rates $\kappa_\pm = \kappa/2$ and one 'dark' mode $D = \frac{1}{\sqrt{2}}(b_1 - b_2)$ at frequency $\omega_{\mathrm{D}} = \Delta$ with a dissipation rate $\kappa_{\mathrm{D}} = \Gamma$. Notice that the bright modes are formed from the superposition of both the optical and the acoustic modes whereas the dark mode lacks an optical mode component, meaning that it does not couple to light. The dynamics of such a system, and the existence of such bright and dark modes, has been explored in an electromechanical system using a GHz frequency microwave resonator strongly coupled to two MHz frequency micromechanical oscillators [29]. However, this regime of coupling has not been previously accessible for optomechanical systems.

Extending the Hamiltonian in Eq. (3) to treat the case of a single optical mode coupling to three acoustic modes, we now expect four eigenmodes of the hybridized system seen in Fig. 4a. Of these eigenmodes, the two broad peaks correspond to the bright modes, whereas the two narrow peaks correspond to the dark modes. This analysis leads us to expect the decay rates of these dark modes to approach the mechanical decay rate $\Gamma_{\mathrm{m}} = 2\pi\times$ 67 kHz. However, high-resolution measurements of such modes at the highest control laser powers (seen in Fig. 4b.iv) reveal decay rates $\Gamma_{\mathrm{d2}} = 2\pi\ \times 14$ kHz and $\Gamma_{\mathrm{d3}} = 2\pi\ \times 15$ kHz, which are approximately 5 times smaller than the original acoustic dissipation rate Γ_{m}. In other words, spectral measurements suggest that the new dark modes formed as a result of strong coupling have much longer lifetimes than any of the uncoupled modes of the system.

To determine veracity of this counterintuitive result, we performed time-domain ring-down measurements to quantify the lifetime of these dark modes (Fig. 4c). The measured decay time of $\tau_d \sim 10.9$ µs confirms that both eigenmodes, which are hybridized excitations of both light and sound, have lifetimes that are significantly longer than the optical and mechanical lifetimes of the uncoupled system.

black The observed dissipation reduction phenomenon can be understood as a form of coherent cancellation that occurs when mechanical modes—which couple into a common reservoir—become strongly hybridized. To understand this, we note that that the Brillouin-active phonon modes supported by this crystal structure can be viewed as leaky modes that lose energy through coupling (or radiation) to a band of phonon modes within the flat-flat crystal geometry. Hence, it is natural to decompose the total decay rate (Γ) into distinct radiative (Γ_{rad}) and intrinsic (Γ_{int}) contributions, such that $\Gamma = \Gamma_{\mathrm{rad}} + \Gamma_{\mathrm{int}}$. Importantly, this radiation constitutes a common bath, and as such Γ_{rad} will appear as both a decay term and a dissipative coupling [47, 48] between different mechanical modes (see Supplementary Information section V [38]).

In the simple case of two acoustic modes treated above, this would correspond to the addition of an off-diagonal term $-i\Gamma_{\mathrm{rad}}$ linking modes b_1 and b_2. In this case, the resulting decay rate of the dark mode, D, becomes $\kappa_{\mathrm{D}} = (\Gamma - \Gamma_{\mathrm{rad}}) + \kappa\delta^2/2g^2$. If radiative loss was the only decay channel, we would thus find $\kappa_{\mathrm{D}} \to 0$ as g becomes large. In reality, $\kappa_{\mathrm{D}} \to \Gamma_{\mathrm{int}}$, which may be set by surface scattering and absorption due to imperfections in the crystal. At cryogenic temperatures Γ_{int} can be very small within pristine crystals [23, 49], opening the possibility of extremely long-lived dark modes. We note that analogous line-narrowing phenomena due to interference of decay pathways has been investigated in fluorescence spectra of a V-type atomic system [50] as well as in a circuit quantum electrodynamics (cQED) platform [51].

Measurement of the linewidths of the two dark modes as a function of power (Fig. 4d) agrees well with the theoretical description of our system presented above. Theoretical fits to the data, for the case of three phonon modes, were performed by numerically diagonalizing the effective Hamiltonian that includes the radiative coupling terms. Only $\Gamma_{\mathrm{int}} = 2\pi \times 5$ kHz is taken as a fit parameter (see Supplementary Information section V [38]) and is consistent with independent measurements of acoustic damping in quartz crystals at cryogenic temperatures [23, 52]. Note that we observe a larger than expected linewidth of the dark modes at the highest powers, which could be due to a deviation from the linear dependence of g on $\sqrt{P_{\mathrm{in}}}$ (see Supplementary Information section III [38]). Nevertheless, these experiments clearly demonstrate that, through the formation of hybridized modes, multimode strong coupling becomes a powerful tool to dynamically manipulate decoherence pathways in optomechanical systems.

IV. DISCUSSION

These results demonstrate that optomechanical coupling to a multitude of high-frequency, low-loss phonons within BAW resonators present intriguing opportunities for investigating classical and quantum phenomena in the multimode strong coupling regime. Moreover, the time-domain measurements presented in this paper represent an important step towards optical control of bulk acoustic phonons for quantum transduction and the generation of non-classical mechanical states. While our system is already in the quantum-coherent strong-coupling regime necessary to observe quantum effects, a number of improvements can be made to achieve robust quantum control of phonons and realize the aforementioned goals.

First, it is possible to directly initialize such high-frequency (12.6 GHz) phonons in their quantum ground states at temperatures < 1 K by using a standard dilution refrigerator. Decreasing κ by improving mirror reflectivity to 99.99 % and utilizing low-loss crystalline substrates with larger Brillouin gain (such as TeO_2) could enable access to the strong coupling regime at < 100 µW input powers. These improvements, along with low duty-cycle pulsed operation of the control laser with micro-Watt average powers could make operation in dilution refrigerators feasible. More importantly, it would be beneficial to design a fiber-coupled optical cavity system with piezo-tunable crystal position to minimize stray optical reflections as well as to provide enhanced control over coupling to one or more phonon modes.

These improvements could offer avenues for utilizing multimode optomechanical interactions for future applications in quantum information and metrology. For in-

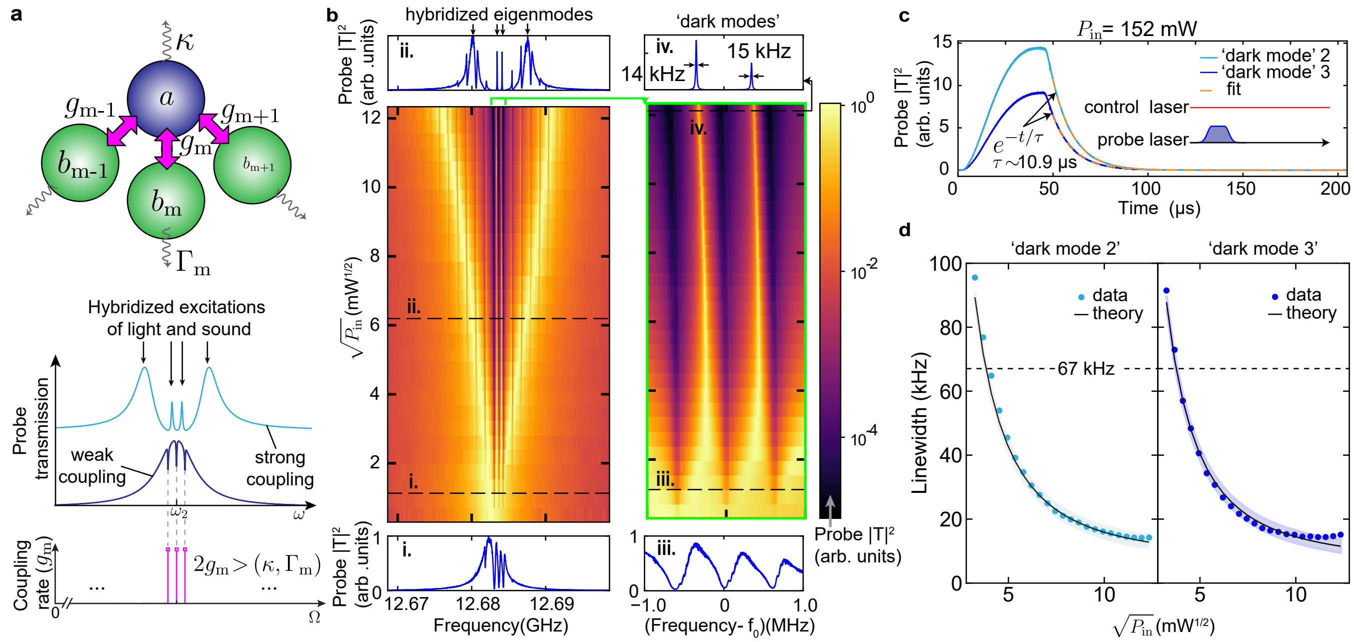

Figure 4. Optomechanical strong coupling to three mechanical modes. (a) Diagram of linearized optomechanical coupling between an optical mode and three acoustic modes (top), corresponding expected spectra of probe laser transmission in the weak and strong coupling regime (middle), and the coupling rate under a strong laser drive (bottom). Strong coupling between an optical mode and three acoustic modes gives rise to four hybridized excitations of light and sound with two narrow resonances corresponding to optical 'dark' modes and the two broad resonances corresponding to optical 'bright' modes. (b) Probe laser transmission spectra taken at various P_{in}. The right panel shows a zoom-in of this spectra around frequency $f_o = 12.684$ GHz. Lower and upper panels (inset **i-iv**) show spectra in the regimes of weak and strong coupling, respectively. In the strongly coupled case (insets **ii** and **iv**), two narrow resonances are observed, corresponding to the optomechanical dark modes. (c) Time-domain measurement of dark modes. Inset shows the pulse sequence for the control and probe lasers. (d) Measured linewidth of the two dark modes at various control laser powers and fits to theory with $\Gamma_{\text{int}}/2\pi = 5$ kHz as described in the main text. The shaded region corresponds to the theoretically-predicted linewidth of the two dark modes when we vary the fit parameter $\Gamma_{\text{int}}/2\pi$ from 3 kHz to 7 kHz.

stance, it may be possible to adiabatically transfer quantum optical states, such as single-photons, to the long-lived dark states for quantum information storage. Moreover, it may be possible to use the nontrivial mode hybridization to generate entangled mechanical states of the resonator by the simultaneously swapping optical excitations to multiple strongly coupled acoustic modes [53]. In addition, as shown by the line-narrowing phenomena we observed, strong coupling between light and acoustic modes within BAW resonators could be used to explore and mitigate acoustic dissipation mechanisms. More generally, it has been shown that acoustic waves within BAW resonators couple strongly to a variety of other quantum systems such as superconducting qubits [54], defect centers [55], and microwave fields [9]. Therefore, deterministic control of bulk acoustic waves using light in the strong coupling regime could be a valuable tool for manipulating quantum information and exploring physical phenomena in hybrid quantum systems.

ACKNOWLEDGMENTS

The authors thank Jack G. E. Harris, Robert J. Schoelkopf, and Liang Jiang for insightful discussions regarding coherent phenomena and for generous contribution of technical expertise and experimental resources. We also thank Luke Burkhart, Vijay Jain, and Yizhi Luo for helpful discussions and valuable feedback. This work was initially supported by the U.S. Office of Naval Research under award number N00014-17-1-2514 and completed under U.S. Department of Energy, Office of Science through award number DE-SC0019406. Y.C. was also supported by the Army Research Office under award number W911NF-14-1-0011. E.A.K. received support from the Packard Fellowship for Science and Engineering. N.T.O. acknowledges support from the National Science Foundation Graduate Research Fellowship under Grant number DGE1122492. The authors of this paper are contributors to patent application no. 62/465101 related to Bulk Crystalline Optomechanics, which was submitted by Yale University.

Author contributions: P.K., Y.C., and E.A.K. performed the experiments under supervision of P.T.R..

P.K., Y.C., and D.M. analyzed the data and developed analytical theory under the guidance of P.T.R.. P.K. designed and built the experimental apparatus to perform the measurement with support from Y.C. and P.T.R.. E.A.K., N.T.O., and S.G. aided in the development of experimental techniques. All authors participated in the writing of this manuscript. P.K and Y.C. contributed equally to this work.

Competing interests: The authors declare that they have no competing interests.

Data and materials availability: All data needed to evaluate the conclusions in the paper are present in the paper and/or the Supplementary Materials. Additional data available from authors upon request.

[1] M. Aspelmeyer, T. J. Kippenberg, and F. Marquardt, "Cavity optomechanics," Rev. Mod. Phys. **86**, 1391–1452 (2014).

[2] M. Mirhosseini, A. Sipahigil, M. Kalaee, and O. Painter, "Superconducting qubit to optical photon transduction," Nature **588**, 599–603 (2020).

[3] R. D. Delaney, M. D. Urmey, S. Mittal, B. M. Brubaker, J. M. Kindem, P. S. Burns, C. A. Regal, and K. W. Lehnert, "Superconducting-qubit readout via low-backaction electro-optic transduction," Nature **606**, 489–493 (2022).

[4] V. Fiore, Y. Yang, M. C. Kuzyk, R. Barbour, L. Tian, and H. Wang, "Storing optical information as a mechanical excitation in a silica optomechanical resonator," Phys. Rev. Lett. **107**, 133601 (2011).

[5] K. Stannigel, P. Komar, S. Habraken, S. Bennett, M. D. Lukin, P. Zoller, and P. Rabl, "Optomechanical quantum information processing with photons and phonons," Phys. Rev. Lett. **109**, 013603 (2012).

[6] H. J. Kimble, "The quantum internet," Nature **453**, 1023 (2008).

[7] P. Rabl, P. Cappellaro, M. G. Dutt, L. Jiang, J. Maze, and M. D. Lukin, "Strong magnetic coupling between an electronic spin qubit and a mechanical resonator," Physical Review B **79**, 041302 (2009).

[8] A. D. O'Connell, M. Hofheinz, M. Ansmann, R. C. Bialczak, M. Lenander, E. Lucero, M. Neeley, D. Sank, H. Wang, M. Weides, *et al.*, "Quantum ground state and single-phonon control of a mechanical resonator," Nature **464**, 697–703 (2010).

[9] X. Han, C.-L. Zou, and H. X. Tang, "Multimode strong coupling in superconducting cavity piezoelectromechanics," Phys. Rev. Lett. **117**, 123603 (2016).

[10] K. Stannigel, P. Rabl, A. S. Sørensen, P. Zoller, and M. D. Lukin, "Optomechanical transducers for long-distance quantum communication," Phys. Rev. Lett. **105**, 220501 (2010).

[11] K. Lee, B. Sussman, M. Sprague, P. Michelberger, K. Reim, J. Nunn, N. Langford, P. Bustard, D. Jaksch, and I. Walmsley, "Macroscopic non-classical states and terahertz quantum processing in room-temperature diamond," Nat. Photonics **6**, 41–44 (2012).

[12] Y.-D. Wang and A. A. Clerk, "Using interference for high fidelity quantum state transfer in optomechanics," Phys. Rev. Lett. **108**, 153603 (2012).

[13] K. Hammerer, M. Wallquist, C. Genes, M. Ludwig, F. Marquardt, P. Treutlein, P. Zoller, J. Ye, and H. J. Kimble, "Strong coupling of a mechanical oscillator and a single atom," Phys. Rev. Lett. **103**, 063005 (2009).

[14] J. P. Reithmaier, G. Sek, A. Löffler, C. Hofmann, S. Kuhn, S. Reitzenstein, L. Keldysh, V. Kulakovskii, T. Reinecke, and A. Forchel, "Strong coupling in a single quantum dot–semiconductor microcavity system," Nature **432**, 197 (2004).

[15] S. Gröblacher, K. Hammerer, M. R. Vanner, and M. Aspelmeyer, "Observation of strong coupling between a micromechanical resonator and an optical cavity field," Nature **460**, 724–727 (2009).

[16] E. Verhagen, S. Deléglise, S. Weis, A. Schliesser, and T. J. Kippenberg, "Quantum-coherent coupling of a mechanical oscillator to an optical cavity mode," Nature **482**, 63–67 (2012).

[17] M. Eichenfield, J. Chan, R. M. Camacho, K. J. Vahala, and O. Painter, "Optomechanical crystals," Nature **462**, 78 (2009).

[18] J. Chan, T. M. Alegre, A. H. Safavi-Naeini, J. T. Hill, A. Krause, S. Gröblacher, M. Aspelmeyer, and O. Painter, "Laser cooling of a nanomechanical oscillator into its quantum ground state," Nature **478**, 89–92 (2011).

[19] R. Riedinger, S. Hong, R. A. Norte, J. A. Slater, J. Shang, A. G. Krause, V. Anant, M. Aspelmeyer, and S. Gröblacher, "Non-classical correlations between single photons and phonons from a mechanical oscillator," Nature **530**, 313–316 (2016).

[20] G. Enzian, M. Szczykulska, J. Silver, L. Del Bino, S. Zhang, I. A. Walmsley, P. Del'Haye, and M. R. Vanner, "Observation of brillouin optomechanical strong coupling with an 11 ghz mechanical mode," Optica **6**, 7–14 (2019).

[21] S. Hunklinger and W. Arnold, "Ultrasonic properties of glasses at low temperatures," Phys. Acoustics **12**, 155–215 (1976).

[22] O. Arcizet, R. Rivière, A. Schliesser, G. Anetsberger, and T. J. Kippenberg, "Cryogenic properties of optomechanical silica microcavities," Phys. Rev. A **80**, 021803 (2009).

[23] W. Renninger, P. Kharel, R. Behunin, and P. Rakich, "Bulk crystalline optomechanics," Nat. Phys. **14**, 601–607 (2018).

[24] Q. Lin, J. Rosenberg, D. Chang, R. Camacho, M. Eichenfield, K. J. Vahala, and O. Painter, "Coherent mixing of mechanical excitations in nano-optomechanical structures," Nat. Photonics **4**, 236 (2010).

[25] C. Dong, V. Fiore, M. C. Kuzyk, and H. Wang, "Optomechanical dark mode," Science **338**, 1609–1613 (2012).

[26] G. Heinrich, M. Ludwig, J. Qian, B. Kubala, and F. Marquardt, "Collective dynamics in optomechanical arrays," Phys. Rev. Lett. **107**, 043603 (2011).

[27] H. Xu, D. Mason, L. Jiang, and J. Harris, "Topological energy transfer in an optomechanical system with exceptional points," Nature **537**, 80 (2016).

[28] F. Ruesink, M.-A. Miri, A. Alu, and E. Verhagen, "Nonreciprocity and magnetic-free isolation based on optome-

chanical interactions," Nat. Commun. **7**, 13662 (2016).

[29] F. Massel, S. U. Cho, J.-M. Pirkkalainen, P. J. Hakonen, T. T. Heikkilä, and M. A. Sillanpää, "Multimode circuit optomechanics near the quantum limit," Nat. Commun. **3**, 987 (2012).

[30] V. Peano, C. Brendel, M. Schmidt, and F. Marquardt, "Topological phases of sound and light," Phys. Rev. X **5**, 031011 (2015).

[31] H. Xu, L. Jiang, A. A. Clerk, and J. G. E. Harris, "Nonreciprocal control and cooling of phonon modes in an optomechanical system," Nature **568**, 65–69 (2019).

[32] M. J. Weaver, D. Newsom, F. Luna, W. Löffler, and D. Bouwmeester, "Phonon interferometry for measuring quantum decoherence," Phys. Rev. A **97**, 063832 (2018).

[33] L. M. d. Lépinay, C. F. Ockeloen-Korppi, M. J. Woolley, and M. A. Sillanpää, "Quantum mechanics–free subsystem with mechanical oscillators," Science **372**, 625–629 (2021).

[34] S. Kotler, G. A. Peterson, E. Shojaee, F. Lecocq, K. Cicak, A. Kwiatkowski, S. Geller, S. Glancy, E. Knill, R. W. Simmonds, J. Aumentado, and J. D. Teufel, "Direct observation of deterministic macroscopic entanglement," Science **372**, 622–625 (2021).

[35] M. Ludwig and F. Marquardt, "Quantum many-body dynamics in optomechanical arrays," Phys. Rev. Lett. **111**, 073603 (2013).

[36] M. J. Hartmann, "Quantum simulation with interacting photons," J. Opt. **18**, 104005 (2016).

[37] P. Kharel, G. I. Harris, E. A. Kittlaus, W. H. Renninger, N. T. Otterstrom, J. G. Harris, and P. T. Rakich, "High-frequency cavity optomechanics using bulk acoustic phonons," Science Advances **5**, 1–9 (2019).

[38] See Supplemental Material at [URL will be inserted by publisher] for additional experimental details and references 56-61.

[39] S. Weis, R. Rivière, S. Deléglise, E. Gavartin, O. Arcizet, A. Schliesser, and T. J. Kippenberg, "Optomechanically induced transparency," Science **330**, 1520–1523 (2010).

[40] A. H. Safavi-Naeini, D. Van Thourhout, R. Baets, and R. Van Laer, "Controlling phonons and photons at the wavelength scale: integrated photonics meets integrated phononics," Optica **6**, 213–232 (2019).

[41] S. M. Meenehan, J. D. Cohen, G. S. MacCabe, F. Marsili, M. D. Shaw, and O. Painter, "Pulsed excitation dynamics of an optomechanical crystal resonator near its quantum ground state of motion," Physical Review X **5**, 041002 (2015).

[42] A. H. Safavi-Naeini, J. Chan, J. T. Hill, S. Gröblacher, H. Miao, Y. Chen, M. Aspelmeyer, and O. Painter, "Laser noise in cavity-optomechanical cooling and thermometry," New Journal of Physics **15**, 035007 (2013).

[43] R. Riedinger, A. Wallucks, I. Marinković, C. Löschnauer, M. Aspelmeyer, S. Hong, and S. Gröblacher, "Remote quantum entanglement between two micromechanical oscillators," Nature **556**, 473–477 (2018).

[44] D. Pinnow and T. Rich, "Development of a calorimetric method for making precision optical absorption measurements," Applied optics **12**, 984–992 (1973).

[45] R. Zeller and R. Pohl, "Thermal conductivity and specific heat of noncrystalline solids," Physical Review B **4**, 2029 (1971).

[46] Y. Chu, P. Kharel, W. H. Renninger, L. D. Burkhart, L. Frunzio, P. T. Rakich, and R. J. Schoelkopf, "Quantum acoustics with superconducting qubits," Science **358**, 199–202 (2017).

[47] A. Metelmann and A. A. Clerk, "Nonreciprocal photon transmission and amplification via reservoir engineering," Phys. Rev. X **5**, 021025 (2015).

[48] K. Fang, J. Luo, A. Metelmann, M. H. Matheny, F. Marquardt, A. A. Clerk, and O. Painter, "Generalized nonreciprocity in an optomechanical circuit via synthetic magnetism and reservoir engineering," Nat. Phys. **13**, 465–471 (2017).

[49] S. Galliou, M. Goryachev, R. Bourquin, P. Abbé, J. P. Aubry, and M. E. Tobar, "Extremely low loss phonon-trapping cryogenic acoustic cavities for future physical experiments," Sci. Rep. **3**, 2132 (2013).

[50] P. Zhou and S. Swain, "Quantum interference in resonance fluorescence for a driven v atom," Phys. Rev. A **56**, 3011 (1997).

[51] N. M. Sundaresan, Y. Liu, D. Sadri, L. J. Szőcs, D. L. Underwood, M. Malekakhlagh, H. E. Türeci, and A. A. Houck, "Beyond strong coupling in a multimode cavity," Phys. Rev. X **5**, 021035 (2015).

[52] P. Kharel, Y. Chu, M. Power, W. H. Renninger, R. J. Schoelkopf, and P. T. Rakich, "Ultra-high-q phononic resonators on-chip at cryogenic temperatures," APL Photonics **3**, 066101 (2018).

[53] M. J. Weaver, F. Buters, F. Luna, H. Eerkens, K. Heeck, S. de Man, and D. Bouwmeester, "Coherent optomechanical state transfer between disparate mechanical resonators," Nature communications **8**, 824 (2017).

[54] Y. Chu, P. Kharel, T. Yoon, L. Frunzio, P. T. Rakich, and R. J. Schoelkopf, "Creation and control of multi-phonon Fock states in a bulk acoustic-wave resonator," Nature **563**, 666–670 (2018).

[55] E. MacQuarrie, T. Gosavi, A. Moehle, N. Jungwirth, S. Bhave, and G. Fuchs, "Coherent control of a nitrogen-vacancy center spin ensemble with a diamond mechanical resonator," Optica **2**, 233–238 (2015).

[56] D. F. Walls and G. J. Milburn, *Quantum optics* (Springer Science & Business Media, 2007).

[57] F. Marquardt, J. P. Chen, A. A. Clerk, and S. M. Girvin, "Quantum Theory of Cavity-Assisted Sideband Cooling of Mechanical Motion," Physical Review Letters **99**, 093902 (2007).

[58] H. J. Carmichael, "Quantum trajectory theory for cascaded open systems," Physical Review Letters **70**, 2273–2276 (1993).

[59] A. A. Clerk, M. H. Devoret, S. M. Girvin, F. Marquardt, and R. J. Schoelkopf, "Introduction to quantum noise, measurement, and amplification," Reviews of Modern Physics **82**, 1155–1208 (2010).

[60] D. Cardimona, M. Raymer, and C. Stroud Jr, "Steady-state quantum interference in resonance fluorescence," Journal of Physics B: Atomic and Molecular Physics **15**, 55 (1982).

[61] E. Nichelatti and G. Salvetti, "Spatial and spectral response of a Fabry–Perot interferometer illuminated by a Gaussian beam," Applied Optics **34**, 4703–4712 (1995).